BIOLOGICALLY INSPIRED TRANSPORT OF SOLID SPHERICAL NANOPARTICLES IN AN ELECTRICALLY-CONDUCTING VISCOELASTIC FLUID WITH HEAT TRANSFER

by

Ahmed ZEESHAN[a*], Muhammad M. BHATTI[b], Nouman IJAZ[a], Osman A. BEG[c], and Ali KADIR[d]

[a] Department of Mathematics and Statistics, International Islamic University, Islamabad, Pakistan
[b] Shanghai Institute of Applied Mathematics and Mechanics, Shanghai University, Shanghai, China
[c] Fluid Mechanics and Propulsion, Aeronautical/Mechanical Engineering Department, School of Computing, Science and Engineering, Newton Building, University of Salford, Manchester, UK
[d] Materials and Corrosion, Aeronautical/Mechanical Engineering Department, School of Computing, Science and Engineering, Newton Building, University of Salford, Manchester, UK

Original scientific paper
https://doi.org/10.2298/TSCI180706324Z

Bio-inspired pumping systems exploit a variety of mechanisms including peristalsis to achieve more efficient propulsion. Non-conducting, uniformly dispersed, spherical nanosized solid particles suspended in viscoelastic medium forms a complex working matrix. Electromagnetic pumping systems often employ complex working fluids. A simulation of combined electromagnetic bio-inspired propulsion is observed in the present article. Currents formation has increasingly more applications in mechanical and medical industry. A mathematical study is conducted for MHD pumping of a bi-phase nanofluid coupled with heat transfer in a planar channel. Two-phase model is employed to separately identity the effects of solid nanoparticles. Base fluid employs Jeffery's model to address viscoelastic characteristics. The model is simplified using long wavelength and creeping flow approximations. The formulation is taken to wave frame and non-dimensionalise the equations. The resulting boundary value problem is solved analytically, and exact expressions are derived for the fluid velocity, particulate velocity, fluid-particle temperature, fluid and particulate volumetric flow rates, axial pressure gradient and pressure rise. The influence of volume fraction density, Prandtl number, Hartmann number, Eckert number, and relaxation time on flow and thermal characteristics is evaluated in detail. The axial flow is accelerated with increasing relaxation time and greater volume fraction whereas it is decelerated with greater Hartmann number. Both fluid and particulate temperature are increased with increment in Eckert and Prandtl numbers, whereas it is reduced when the volume fraction density increases. With increasing Hartmann number pressure rise is reduced.

Key words: *nanosized particles, two-phase model, heat transfer, MHD, bioinspired pumps*

Introduction

In recent decades, bioinspired pumping mechanisms have been increasingly deployed in industrial systems owing to their superiority in efficiency and sustainability. These systems employ complex biological characteristics including ciliated walls, variable stiffness

* Corresponding author, e-mail: ahmad.zeeshan@iiu.edu.pk

and wall deformability, adaptive healing, surface tension and many other intriguing features [1]. One of the most efficient and frequently deployed mechanisms of biological transport is peristalsis. This involves the propulsion of physiological fluids *via* rhythmic contraction of the walls of a vessel. In particular, peristaltic pumping finds significant applications in finger pumps, roller pumps, transport of hazardous wastes and also medical drug delivery. Early studies of the fabrication and engineering performance of peristaltic pumps for Newtonian viscous fluids were conducted by Latham [2]. Numerous analytical and computational investigations of peristaltic hydrodynamics have subsequently been reported. These have also featured supplementary phenomena including non-Newtonian effects, heat and mass transfer, nanofluids, *etc*. Representative studies include [3-10]. These studies have generally investigated peristaltic flow with the assumption of wave on the walls of the channel has a much greater wavelength when compared with amplitude of the wave and the transmission of fluid is slow results in low Reynolds number *i. e.* they have employed the so-called lubrication theory. Investigations on peristaltic flow with heat transfer have been reported by Ramesh and Devakar [11] who studied the effects of heat on peristaltic flow in a porous channel with perpendicular magnetic field. Bhatti, *et al*. [12] analysed effects of thermal radiation on the two-phase viscous fluid with constant magnetic field. Flow was induced by metachronal wave. Further studies include Vajravelu *et al*. [13] Mekheimer and Abd Elmaboud [14], Srinivas and Kothandapani [15] and therein.

The MHD concern the interaction of static or alternating magnetic fields with electrically-conducting fluids. It arises in diverse applications including electromagnetics casting, plasma flows, cooling of nuclear reactors, magnetic materials processing. The MHD peristaltic flows combine the flow control features of MHD with the efficient propulsive features of peristalsis. Such flows are present in bioinspired MHD medical pumps where very effective transport of different biological fluids can be achieved. These pumps also include continuous and non-pulsating modes intrinsic to a variety of complex geometrical designs. Extensive studies of MHD peristaltic flows have been communicated and have demonstrated the excellent regulation of bolus growth which is possible with the careful implementation of magnetic fields. Examples of such studies include Misra *et al*. [16] for viscoelastic fluid in a channel with stretching walls and Tripathi *et al*. [17] for Newtonian conducting fluids.

In certain energy and medical engineering applications, two-phase fluids may also arise. These generally comprise particles suspended in a fluid. Bi-phase fluid models represent a good approximation for blood (erythrocytes in plasma), Trowbridge [18], biotechnological suspensions, Beg *et al*. [19] and also doped working fluids in MHD generators. Some relevant examples are included in [20-30]. Several of these studies have also considered heat transfer.

The present article investigates the biologically inspired peristaltic transport of magneto-bi-phase non-Newtonian (viscoelastic) fluid and its heat transfer through a planar channel. Generation of internal energy due to viscosity is also included. The corresponding flow equations are formulated for fluid and particulate phase. Law of conservation of mass, linear momentum (fluid and particle phases) and thermal energy along with Ohm's law are employed. Equations are simplified with the help of lubrication theory. Exact solutions are achieved. The rise in pressure is evaluated using numerical integration in MATHEMATICA. Results are visualized through graphs for the influence of a number of emerging parameters. Streamlines are also plotted to observe boluses. The computations provide a deeper insight into the transport phenomena in magnetic biopumps using a more realistic working fluid model (viscoelastic dusty model).

Modeling and dimensional analysis

Assume, MHD peristaltic pumping of a dusty (fluid-particulate) viscoelastic fluid in a 2-D planar channel. Viscoelastic characteristics of the dusty fluid are simulated with the Jeffery's model. The walls of the channel are considered to be electrically-insulated and a magnetic field with constant strength B_0 is applied externally. We have selected rectangular co-ordinates in a way that $\tilde{x}$-axis is taken parallel to centre line, while, $\tilde{y}$-axis is normal to the flow as seen through systemic geometry displayed in fig. 1. Hall current, magnetic-induction and ion slip effects are neglected. The particles are small spherical, have uniform size and in thermal equilibrium with the viscoelastic liquid. The equation describing peristaltic wave on the wall is [31]:

$$\tilde{h}\left(\tilde{x},\tilde{t}\right)=\tilde{a}\left[1+\tilde{q}\sin\frac{2\pi}{\lambda}\left(\tilde{x}-\tilde{c}\tilde{t}\right)\right],\ \tilde{q}=\frac{\tilde{b}}{\tilde{a}} \tag{1}$$

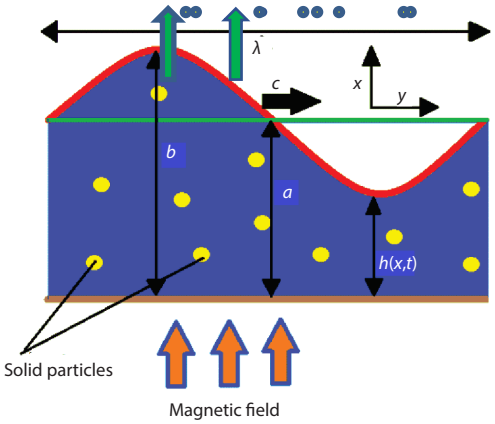

Figure 1. Geometry of problem showing half channel

The governing equations for mass conservation and momentum conservation for both the liquid phase and particulate phase are formulation using continuum mechanics as Mekheimer *et al*. [32].

– Fluid phase:

$$\nabla V_{\mathrm{f}}=0 \tag{2}$$

$$\left(1-C\right)\rho_{\mathrm{f}}\frac{DV_{\mathrm{f}}}{Dt}=-\left(1-C\right)\nabla P+\left(1-C\right)\nabla S+\frac{Ccd}{\varpi v}\left(V_{\mathrm{p}}-V_{\mathrm{f}}\right)+JB \tag{3}$$

– Particulate phase:

$$\nabla V_{\mathrm{p}}=0 \tag{4}$$

$$\left(1-C\right)\rho_{\mathrm{p}}\frac{DV_{\mathrm{p}}}{Dt}=-\left(1-C\right)\nabla P-\frac{Ccd}{\varpi_{v}}\left(V_{\mathrm{p}}-V_{\mathrm{f}}\right) \tag{5}$$

The drag coefficient of the suspension in terms of Reynolds number for slowly moving fluid can be described by the following mathematical relations [33]:

$$cd=\frac{24}{\mathrm{Re}}\left(1+\frac{3}{16}\mathrm{Re}\right) \tag{6}$$

The tensor describing the shear and normal stresses for Jeffrey's viscoelastic fluid model may be defined, Bhatti *et al*. [34]:

$$\mathbf{S}=\frac{\mu_s}{1+\lambda_1}\left(\dot{\gamma}+\lambda_2\ddot{\gamma}\right) \tag{7}$$

Equations for heat transfer by the fluid and particles for suspension with the assumption that particles are not good conductor of heat are (Bhatti *et al*. [35]):

$$\left(1-C\right)\rho_{\mathrm{f}}cp_{\mathrm{f}}\frac{\mathrm{D}\theta_{\mathrm{f}}}{\mathrm{D}t}=\left(1-C\right)\nabla\left(k\nabla\theta_{\mathrm{f}}\right)+\frac{\rho_{\mathrm{p}}c_pC}{\varpi_T}\left(\theta_{\mathrm{p}}-\theta_{\mathrm{f}}\right)+\frac{Ccd}{\varpi_{v}}\left(\tilde{u}_{\mathrm{f}}-\tilde{u}_{\mathrm{p}}\right)^2+\Phi \tag{8}$$

$$(1-C)\rho_{\mathrm{p}} cp_{\mathrm{p}} \frac{D\theta_{\mathrm{p}}}{\mathrm{D}t} = -\frac{\rho_{\mathrm{p}} c_p C}{\varpi_{\boldsymbol{T}}}\left(\theta_{\mathrm{p}} - \theta_{\mathrm{f}}\right) \tag{9}$$

where Φ the viscous forces converted to internal energy called viscous dissipation:

$$\Phi = (\mathrm{S}\nabla)V \tag{10}$$

Equations are transformed in wave frame by horizontal velocity with wave speed $u' = \tilde{u} - \mathrm{c}$ and $x' = \tilde{x} - \tilde{c}\tilde{t}$.

After introducing non-dimensional parameters and using lubrication theory, eqs. (2)-(10) takes the form:

$$\frac{\mathrm{d}p}{\mathrm{d}x} = \frac{1}{1+\lambda_1}\frac{\partial^2 u_{\mathrm{f}}}{\partial y^2} - \mathrm{M}^2\left(u_{\mathrm{f}} + 1\right) + \frac{NC}{\left(1-C\right)}\left(u_{\mathrm{p}} - u_{\mathrm{f}}\right) \tag{11}$$

$$\frac{1}{\mathrm{Pr}}\frac{\partial^2 \theta_{\mathrm{f}}}{\partial y^2} + \mathrm{Ec}\left(\frac{\partial u_{\mathrm{f}}}{\partial y}\right)^2 + \frac{\mathrm{Ec}}{N\left(1-C\right)}\left(\frac{\mathrm{d}p}{\mathrm{d}x}\right)^2 = 0 \tag{12}$$

$$\frac{\mathrm{d}p}{\mathrm{d}x} = N\left(u_{\mathrm{f}} - u_{\mathrm{p}}\right) \tag{13}$$

$$\theta_{\mathrm{f}} = \theta_{\mathrm{p}} \tag{14}$$

where it is assumed that x is of order of wave length λ, y – equivalent to order of amplitude of wave a. Similarly, horizontal velocity u proportional to speed of wave c. Temperature θ is defined as ratio of differences of temperature from any wall and between both walls. The Ec, N, Pr, and M, are Eckert number, drag coefficient, Prandtl number, and Hartmann's number, respectively.

On the wall $y = h$ velocity and temperature take the form:

$$_{\mathrm{f}} = -1, \quad _{\mathrm{f}} = 1 \tag{15}$$

where

$$h = 1 + \phi \sin 2\pi x \tag{16}$$

and at $y = 0$.

$$u_{\mathrm{f}}' = \theta_{\mathrm{f}} = 0 \tag{17}$$

Analytical solutions

The exact solutions of eqs. (11)-(14) is obtained under boundary conditions (15)-(17). Equation (13) is used in eq. (11) to get a uncouple both equations. Resultant equation by taking as constant with respect to y reduced to linear second order non-homogenous differential equation. Using complimentary and particular solution uf becomes:

$$u_f = -1 + \left[\frac{\frac{\mathrm{d}p}{\mathrm{d}x}\left(1 - \cosh\left[\mathrm{M}y\sqrt{1+\lambda_1}\right]\mathrm{sech}\left[h\mathrm{M}\sqrt{1+\lambda_1}\right]\right)}{\left(-1+C\right)\mathrm{M}^2}\right] \tag{18}$$

Using u_{f} in eq. (13) we get:

$$u_{\mathrm{p}} = \frac{1}{\left(-1+C\right)\mathrm{M}^2}\frac{\mathrm{d}p}{\mathrm{d}x}\left[-\left(-1+c\right)\mathrm{M}^2\left(1 + N\frac{\mathrm{d}p}{\mathrm{d}x}\right)\cosh \mathrm{M}y\sqrt{1+\lambda_1}\,\mathrm{sech}h\mathrm{M}\sqrt{1+\lambda_1}\right] \tag{19}$$

Solving eq. (12) which is also second order ODE and using eq. (17) we have:

$$\theta_f = \theta_p =$$
$$\left(\begin{array}{l}\operatorname{sech}^2 h\mathrm{M}\sqrt{1+\lambda_1}\left(\begin{array}{l}4(-1+C)^2\mathrm{M}^4 Ny - \mathrm{Ec}\left(\dfrac{\mathrm{d}p}{\mathrm{d}x}\right)^2 \mathrm{Pr}(h-y)\left[-N+2h\mathrm{M}^2\left((-1+C)\mathrm{M}^2+N\right)y\right]+\\ +y\left(\mathrm{Ec}N\left(\dfrac{\mathrm{d}p}{\mathrm{d}x}\right)^2 \mathrm{Pr}+2(-1+C)\mathrm{M}^4\left(2(-1+C)N+\mathrm{Ec}h\left(\dfrac{\mathrm{d}p}{\mathrm{d}x}\right)^2 \mathrm{Pr}(-h+y)\right)\right)\cdot\\ \cdot\cosh 2h\mathrm{M}\sqrt{1+\lambda_1} - \mathrm{Ec}hN\left(\dfrac{\mathrm{d}p}{\mathrm{d}x}\right)^2 \mathrm{Pr}\cos h2y\mathrm{M}\sqrt{1+\lambda_1} + 2\mathrm{Ec}h\mathrm{M}^2 N\left(\dfrac{\mathrm{d}p}{\mathrm{d}x}\right)^2\cdot\\ \cdot\mathrm{Pr}y(-h+y)\lambda_1\end{array}\right)\\ /8(-1+C)^2 h\mathrm{M}^4 N\end{array}\right) \tag{20}$$

The volumetric flow rate is given.

$$Q_{\mathrm{f}} = (1-C)\int_0^h u_{\mathrm{p}}\,\mathrm{d}y \tag{21}$$

$$Q_{\mathrm{p}} = C\int_0^h u_{\mathrm{p}}\,\mathrm{d}y \tag{22}$$

here

$$Q = Q_{\mathrm{f}} + Q_{\mathrm{p}} \tag{23}$$

$$Q = \frac{h}{(C-1)\mathrm{M}^2}\left[(1-C)\mathrm{M}^2 + \frac{\mathrm{d}p}{\mathrm{d}x} + C(1-C)\mathrm{M}^2 N\frac{\mathrm{d}p}{\mathrm{d}x}\right] - \frac{\mathrm{d}p}{\mathrm{d}x}\frac{\tanh h\mathrm{M}\sqrt{1+\lambda_1}}{(-1+C)\mathrm{M}^3\sqrt{1+\lambda_1}} \tag{24}$$

Cracking eq. (24) to get dp/dx, which is linear equation, rearranging eq. (24), by taking dp/dx common and obtaining a relation in terms of Q:

$$\frac{\mathrm{d}p}{\mathrm{d}x} = \frac{(-1+C)\mathrm{M}^3(-h-Q)\sqrt{1+\lambda_1}}{-h\mathrm{M}\sqrt{1+\lambda_1} - Ch\mathrm{M}^3 N\sqrt{1+\lambda_1} + C^2 h\mathrm{M}^3 N\sqrt{1+\lambda_1} + \tanh h\mathrm{M}\sqrt{1+\lambda_1}} \tag{25}$$

Adimensional ΔP can be calculated using relation:

$$\Delta P = \int_0^1 \frac{\mathrm{d}p}{\mathrm{d}x}\,\mathrm{d}x \tag{26}$$

Numerical Integration using MATHEMATICA 10 software is employed to obtain the results of ΔP.

Graphs and discussion

In this section, selected graphical results for the influence of different parameters on the fluid phase and particulate phase are elaborated. We consider the effects of the thermo-physical, non-Newtonian, and magnetic parameters on velocity and temperature profiles, pressure rise and finally bolus dynamics (peristaltic streamline plots for visualizing the trapping mechanism), respectively. Rise or drop in pressure in eq. (26) is estimated using numerical integration MATHEMATICA.

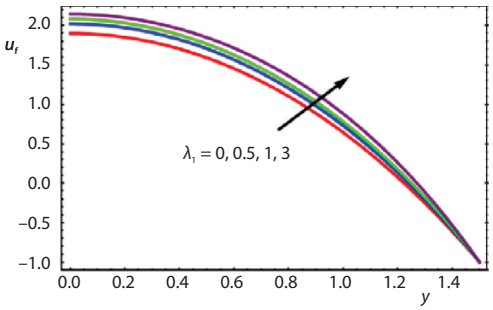

Figure 2. Influence of variation in values of λ_1 on fluid velocity

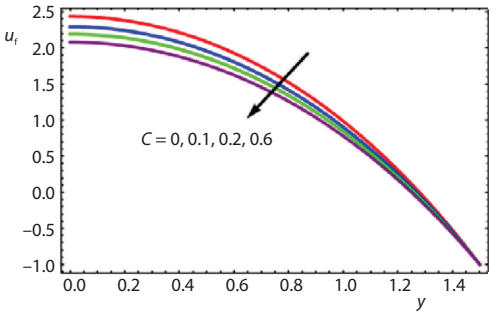

Figure 3. Influence of variation in values of *C* on fluid velocity

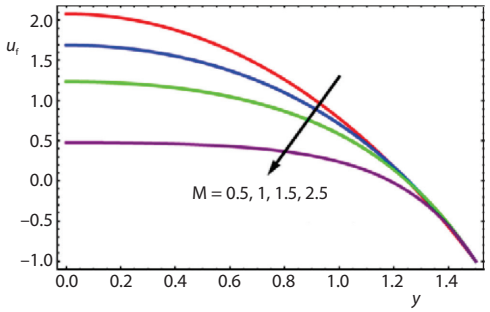

Figure 4. Influence of variation in values of M on fluid velocity

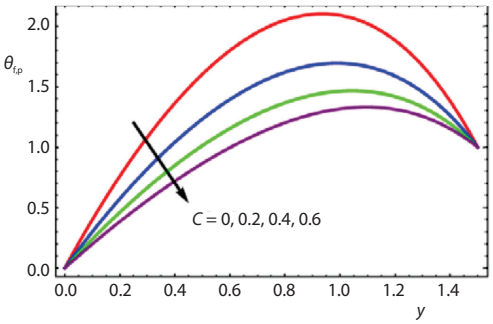

Figure 5. Influence of variation in values of *C* on fluid and particle temperature

Close inspection of fig. 2 reveals that for a Newtonian fluid (vanishing viscoelastic characteristics *i. e.* zero relaxation time, $\lambda_1 = 0$) the fluid velocity declines whereas, for the non-Newtonian scenario $\lambda_1 \neq 0$ the velocity of the fluid is enhanced with greater relaxation time, λ_1. Axial flow is therefore, strongly accelerated with greater viscoelasticity of the working fluid. Figure 3 demonstrates that with increasing values of volume fraction density, *C*, the axial flow is strongly decelerated *i. e.* fluid velocity is decreased. Figure 4 illustrates that the velocity of the fluid decreases when the Hartmann (magnetic body force) parameter increases. When magnetic field is applied it induces a retarding effect via the axial Lorentz MHD body force which serves to decelerate the axial flow. This decreases the fluid phase velocity.

Temperature profile

Figures 5-8 depict the variation of temperature profiles for both the fluid phase and particulate phase. From fig. 5 it is evident that temperatures are suppressed with an increment in the volume fraction density, *C*, since greater concentration of solid particles effectively reduces thermal diffusion in the fluid phase. Figure 6 indicates that temperature increases with an increment in Eckert number since there is greater conversion of kinetic energy to thermal energy via viscous dissipation. Similarly, an increase in Prandtl number enhances temperatures in the regime, as observed in fig. 7. Figure 8 shows that temperature profile increases when the Hartmann number rises. The extra work consumed in dragging the fluid-particle suspension *vs.* magnetic field is released in form of internal energy. This heats the regime and lifts temperatures.

Pumping characteristics

Figures 9-11 illustrates the rise or drop in pressure *vs.* volumetric flow rate *Q*. It can be observed using fig. 9 that pressure drops in the retrograde pumping region, whereas, the opposing response is displayed in the free pumping region and co-pumping region for various val-

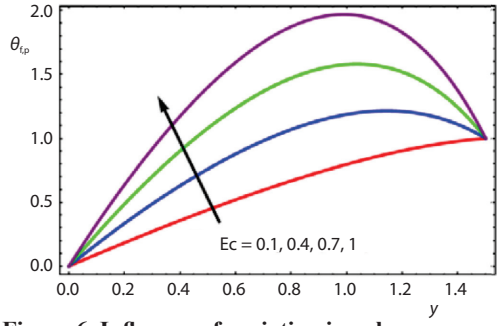

Figure 6. Influence of variation in values of Ec on fluid and particle temperature

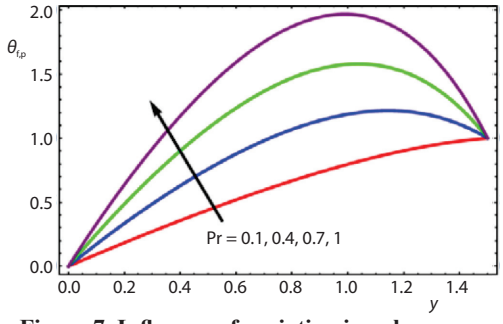

Figure 7. Influence of variation in values of Pr on fluid and particle temperature.

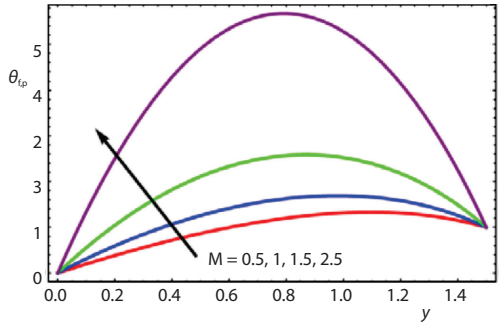

Figure 8. Influence of variation in values of M on fluid and particle temperature

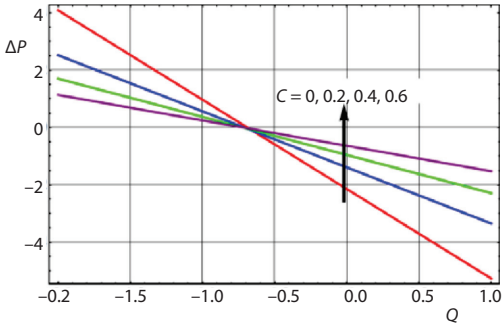

Figure 9. Influence of variation in values of *C* on rise in pressure *vs.* *Q*

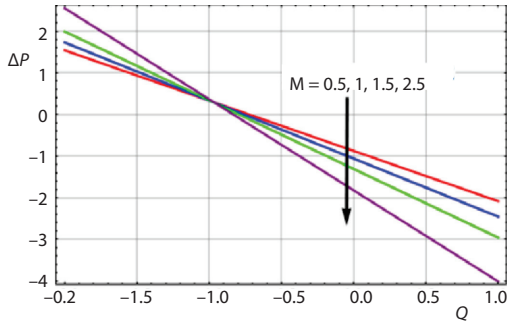

Figure 10. Influence of variation in values of M on rise in pressure *vs.* *Q*

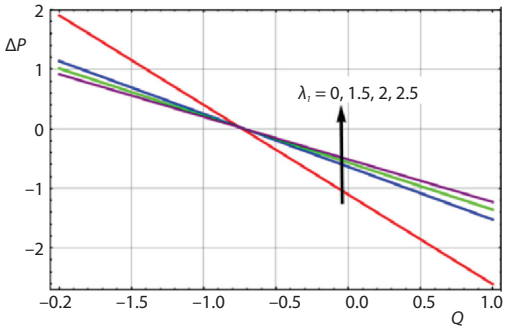

Figure 11. Influence of variation in values of λ_1 on rise in pressure *vs.* *Q*

ues of concentration density C. It is also apparent from fig. 10 that when stronger transverse magnetic field is applied, pressure drops in the co-pumping region and free pumping region, whereas it is enhanced in the retrograde pumping region. In fig. 11 we can see that pressure decreases for $\lambda_1 = 0$, *i. e.* Newtonian fluid, in the retrograde pumping region, whereas the opposite effect is induced in the co-pumping region and free pumping region. Viscoelastic fluids demonstrate the converse behaviour.

Trapping phenomena

Another interesting feature of such flows is trapping phenomena. Streamlines helps to unveil trapping *i. e.* the formation of an internally circulating bolus that is enclosed by stream-

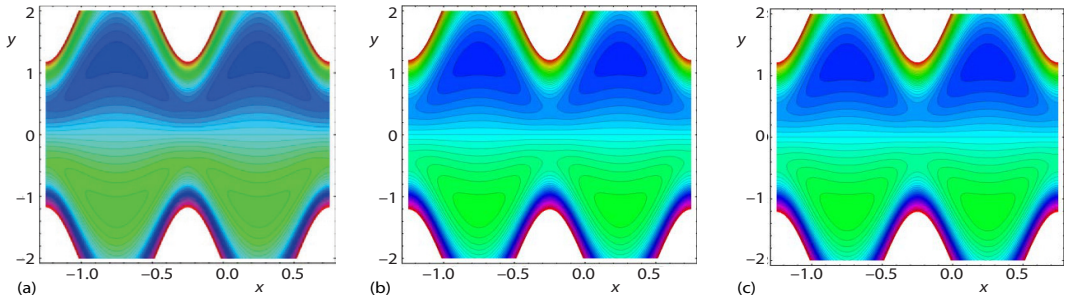

Figure 12. Streamlines for numerous values of C = 0, 0.3, 0.6 (*for color image see journal web site*)

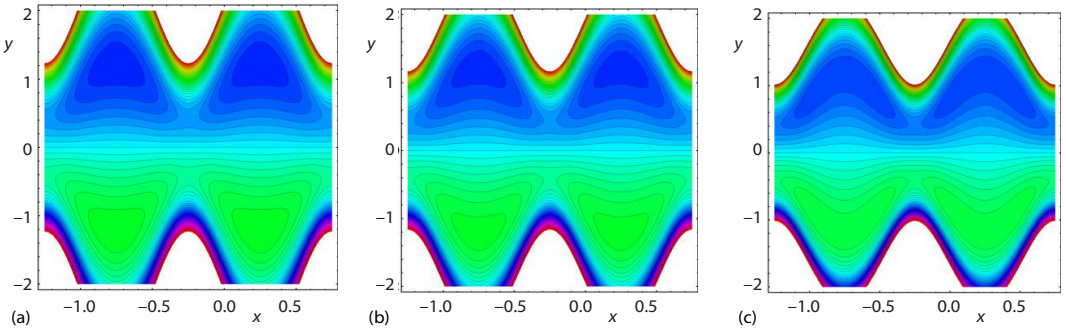

Figure 13. Streamlines for numerous values of M = 0.5, 1.0, 1.5 (*for color image see journal web site*)

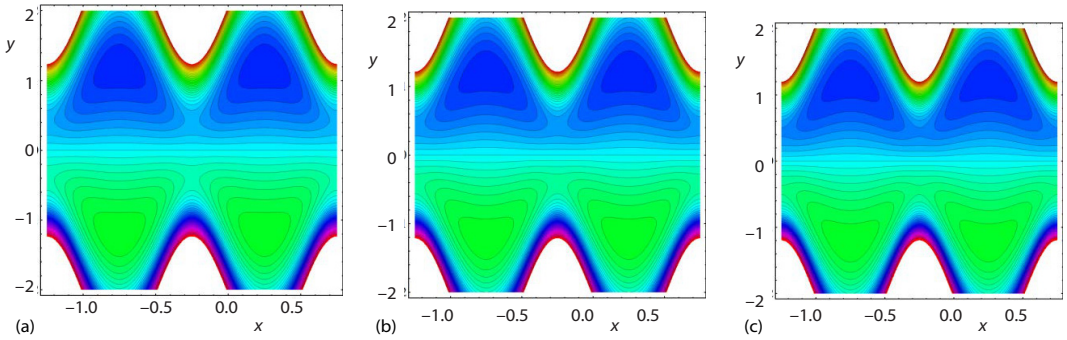

Figure 14. Streamlines for numerous values of λ_1 = 0, 1, 2 (*for color image see journal web site*)

lines. The bolus designates to the volume of the fluid trapped in closed streamline. It can be observed through fig. 12 that when C increases, then the number of boluses also increases whereas the bolus size demises. From fig. 13 it is observed that the number of bolus reduces with increasing values of magnetic parameter M. Figure 14 shows that when λ_1 (relaxation parameter) grows then the bolus count decreases.

Conclusions

Flow and coupled with heat transfer analysis in the biologically inspired peristaltic transport of an electrically-conducting magneto-bi-phase viscoelastic suspension has been studied theoretically in current manuscript. The present study has revealed interesting characteristics of dusty peristaltic bioinspired magnetic pumping systems. Further studies will address slip effects at the walls and will be communicated imminently. A few results are mentioned.

- Numerical computations have shown that velocity of the fluid decreases when the Hartmann (magnetic) number and volume fraction density increases.
- It is found that both fluid and particulate phase temperatures increases with magnetic Hartmann number, Eckert (viscous dissipation) number and Prandtl number.
- Whereas, fluid and particulate phase temperatures are reduced when the volume fraction density increases.
- Increasing viscoelastic relaxation time generates acceleration in the axial flow.
- Increasing volume fraction density results in a reduction in the trapped bolus magnitude whereas the number of boluses increases.
- The present analysis reduces to the Newtonian fluid by taking $\lambda_1 = 0$.

Nomenclature

$\tilde{a}$ – wave amplitude, [m]
B_0 – magnetic field, [NsC^{-1}m^{-1}]
$\tilde{b}$ – width of the channel
C – volume fraction density
$\tilde{c}$ – wave velocity, [ms^{-1}]
c_p – specific heat at constant volume, [Jkg^{-1}K^{-1}]
Ec – Eckert number, [–]
k – thermal conductivity, [Wm^{-1}K^{-1}]
M – Hartmann number, [–]
$\tilde{P}$ – pressure in fixed frame, [Pa]
Pr – Prandtl number, [–]
Q – volume flow rate, [m^{3}s^{-1}]
Re – Reynolds number, [–]
S – drag force
$\mathbf{S}$ – stress tensor, [Nm^{-2}]
$\tilde{t}$ – time, [s]
$\tilde{U}$, $\tilde{V}$ – velocity components in fixed frame, [ms^{-1}]
$\tilde{X}$, $\tilde{Y}$ – Cartesian co-ordinate axis in fixed frame

Greek symbols

γ – shear rate, [s^{-1}]
θ – dimensionless temperature, [–]
λ – wavelength, [m]
λ_1, λ_2 – relaxation time and retardation time
μ_s – viscosity of the fluid, [Nsm^{-2}]
$\bar{\omega}_T$ – thermal equilibrium time
$\bar{\omega}_v$ – relaxation time of the particle
ρ – fluid density, [kgm^{-3}]
ϕ – amplitude ratio

Subscripts

f – fluid phase
p – particulate phase

References

[1] Aboelkassem, Y., *Novel Bioinspired Pumping Models for Microscale Flow Transport*, Dissertation Virginia Technical Institute, Altavista, Va., USA, 2012
[2] Latham, T. W., *Fluid Motions in a Peristaltic Pump*, Dissertation Massachusetts Institute of Technology, Cambridge, Mass., USA, 1966
[3] Pozrikidis, C., A Study of Peristaltic Flow, *Journal of Fluid Mechanics, 180* (1987), July, pp. 515-527
[4] Ahmed, S. E., *et al*., The MHD Mixed Thermo-Bioconvection in Porous Cavity Filled by Oxytactic Microorganisms, *Thermal Science*, *22* (2018), 6B, pp. 2711-2721
[5] Bhatt, S. S., *et al.*, Effects of Heat Transfer during Peristaltic Transport in Non-Uniform Channel with Permeable Walls, *Journal of Heat Transfer*, *139* (2017), 1, 014502
[6] Bohme, G., Friedrich, R., Peristaltic Flow of Viscoelastic Liquids, *Journal of Fluid Mechanics*, *128* (1983), Mar., pp. 109-122
[7] Eldabe, N. T., *et al*., Hall Effects on the Peristaltic Transport of Williamson Fluid through a Porous Medium with Heat and Mass Transfer, *Applied Mathematical Modelling*, *40* (2016) 1, pp. 315-328
[8] Zeeshan, A., *et al*., Analysis of Magnetohydrodynamics Peristaltic Transport of Hydrogen Bubble in Water, *International Journal of Hydrogen Energy*, *43* (2018), 2, pp. 979-985
[9] Siddiqui, A. M., Schwarz, W. H., Peristaltic Flow of a Second-Order Fluid in Tubes, *Journal of Non-Newtonian Fluid Mechanics*, *53* (1994), July, pp. 257-284
[10] Riaz, A., *et al.*, Effects of the Wall Properties on Unsteady Peristaltic Flow of an Eyring-Powell Fluid in a 3-D Rectangular Duct, *International Journal of Biomathematics*, *8* (2015), 6, 1550081
[11] Ramesh, K., Devakar, M., Magnetohydrodynamic Peristaltic Transport of Couple Stress Fluid through Porous Medium in an Inclined Asymmetric Channel with Heat Transfer, *Journal of Magnetism and Magnetic Materials*, *394* (2015), Nov., pp. 335-348

[12] Bhatti, M. M., *et al.*, Heat Transfer with Thermal Radiation on MHD Particle–Fluid Suspension Induced by Metachronal Wave, *Pramana*, *89* (2017), Sept., 48
[13] Vajravelu, K., *et al.*, Peristaltic Flow and Heat Transfer in a Vertical Porous Annulus, with Long Wave Approximation, *International Journal of Non-Linear Mechanics*, *42* (2007) 5, pp. 754-759
[14] Mekheimer, K. S., Abd Elmaboud, Y., Peristaltic Transport of a Particle-Fluid Suspension through a Uniform and Non-Uniform Annulus, *Applied Bionics and Biomechanic*, 5 (2008) 2, pp. 47-57
[15] Srinivas, S., Kothandapani, M., Peristaltic Transport in an Asymmetric Channel with Heat Transfer – A Note, *International Communications in Heat and Mass Transfer*, *35* (2008) 4, pp. 514-522
[16] Misra, J. C., *et al*., A Numerical Model for the Magnetohydrodynamic Flow of Blood in a Porous Channel, *Journal of Mechanics in Medicine and Biology*, *11* (2011), 3, pp. 547-562
[17] Tripathi, D., *et al*., Electro-Magneto-Hydrodynamic Peristaltic Pumping of Couple Stress Biofluids through a Complex Wavy Micro-Channel, *Journal of Molecular Liquids*, *236* (2017), June, pp. 358-367
[18] Trowbridge, E. A., The Fluid Mechanics of Blood: Equilibrium and Sedimentation, *Clinical Physics and Physiological Measurement*, *3* (1982), 4, 249
[19] Beg, T. A., *et al*., Differential Transform Semi-Numerical Analysis of Biofluid-Particle Suspension Flow and Heat Transfer in non-Darcian Porous Media, *Computer Methods in Biomechanics and Biomedical Engineering*, *16* (2013) 8, pp. 896-907
[20] Horng, H. E., *et al.*, Novel Properties and Applications in Magnetic Fluids, *Journal of Physics and Chemistry of Solids*, *62* (2001), 9-10, pp. 1749-1764
[21] Roy, R., *et al*., Unsteady Two-Phase Flow in a Catheterized Artery with Atherosclerosis, *International Journal of Fluid Mechanics Research*, *42* (2015), 4, pp. 334-354
[22] Ijaz, N., *et al*., Heat Transfer Analysis in MHD Flow of Solid Particles in Non-Newtonian Ree-Eyring Fluid due to Peristaltic Wave in A Channel, *Thermal Science*, *23* (2019), 2B, pp. 1017-1026
[23] Srivastava, L. M., Srivastava, V. P., Peristaltic Transport of a Particle-Fluid Suspension, *Journal of Biomechanical Engineering*, *111* (1989), 2, pp. 157-165
[24] Sheikholeslami, M., *et al*., Lorentz Forces Efect on NEPCM Heat Transfer during Solidification in a Porous Energy Storage System, *International Journal of Heat and Mass Transfer*, *127* (2018), Part A, pp. 665-674
[25] Bhatti, M. M., *et al*., Mathematical Modelling of Heat and Mass Transfer Effects on MHD Peristaltic Propulsion of Two-Phase Flow through a Darcy-Brinkman-Forchheimer Porous Medium, *Advanced Powder Technology*, *29* (2018) 5, pp. 1189-1197
[26] Sheikholeslami, M., Rokni, H. B., Magnetic Nanofluid-Flow and Convective Heat Transfer in a Porous Cavity Considering Brownian Motion Effects, *Physics of Fluids*, *30* (2018), 1, 012003
[27] Hassan, M., *et al*., Convective Heat Transfer Flow of Nanofluid in a Porous Medium over Wavy Surface, *Physics Letters A*, *382* (2018), 38, pp. 2749-2753
[28] Sheikholeslami, M., Application of Darcy Law for Nanofluid-Flow in a Porous Cavity under the Impact of Lorentz Forces, *Journal of Molecular Liquids*, *266* (2018), Sept., pp. 495-503
[29] Sheikholeslami, M., Rokni, H. B., The CVFEM for Effect of Lorentz Forces on Nanofluid-Flow in a Porous Complex Shaped Enclosure by Means of Non-Equilibrium Model, *Journal of Molecular Liquids*, *254* (2018), Mar., pp. 446-462
[30] Hassan, M., *et al*., Exploration of Convective Heat Transfer and Flow Characteristics Synthesis by Cu-Ag/Water Hybrid-Nanofluids, *Heat Transfer Research*, *49* (2018), 18, pp. 1837-1848
[31] Zeeshan, A., *et al*., Mathematical Study of Peristaltic Propulsion of Solid-Liquid Multi-Phase Flow with a Biorheological Fluid as the Base Fluid in a Duct, *Chinese Journal of Physics*, *55* (2017) 4, pp. 1596-1604
[32] Mekheimer, K. S., *et al*., Peristaltic Motion of a Particle-Fluid Suspension in a Planar Channel, *International Journal of Theoretical Physics*, *37* (1998), 11, pp. 2895-2920
[33] Chhabra, R. P., *Bubbles, Drops, and Particles in Non-Newtonian Fluids*, CRC press, Boca Raton, Fla., USA, 2006
[34] Bhatti, M. M., *et al*., Simultaneous Effects of Coagulation and Variable Magnetic Field on Peristaltically Induced Motion of Jeffrey Nanofluid Containing Gyrotactic Microorganism, *Microvascular Research*, *110* (2017), Mar., pp. 32-42
[35] Bhatti, M. M., *et al.*, Thermally Developed Peristaltic Propulsion of Magnetic Solid Particles in Biorheological Fluids, *Indian Journal of Physics*, *92* (2018), 4, pp. 423-430

Paper submitted: July 24, 2018
Paper revised: November 23, 2018
Paper accepted: November 24, 2018